



Release of geogenic uranium and arsenic results in water-quality impacts in a subarctic permafrost region of granitic and metamorphic geology

Elliott K. Skierszkan^{a,b,*}, John W. Dockrey^b, K. Ulrich Mayer^a, Roger D. Beckie^a

^a Department of Earth, Ocean and Atmospheric Sciences, University of British Columbia, 2020-2207 Main Mall, Vancouver V6T 1Z4, Canada,

^b Lorax Environmental Services Ltd., 2289 Burrard St, Vancouver V6J 3H9, Canada

ARTICLE INFO

Keywords

Uranium
Arsenic
Water quality
Trace metals
Groundwater
Geogenic contamination
Subarctic
Baseline
Permafrost

ABSTRACT

This study investigates geogenic U and As mobilization in relation to bedrock geology, groundwater geochemistry, and the presence of mineral deposits in the Dawson Range, Yukon, Canada, a remote subarctic region that has drawn recent interest from mining industry. Elevated concentrations of U and As occur through natural weathering processes. For this study we compiled and interpreted a geochemical dataset from the region that includes 1075 rock samples, 365 sediment samples, 3189 surface water samples, and 384 groundwater samples. Median U concentrations exceed the Canadian guideline for the protection of aquatic life of 15 µg/L (long-term exposure) at 8% of 547 surface-water monitoring locations and the maximum observed concentration is 337 µg/L. 39% of monitoring wells have median groundwater U concentrations above this guideline and the maximum observed concentration is 589 µg/L. Uranium mobilization is driven by weathering of granitic and metamorphic bedrock that has contents near or slightly above the average upper crustal abundance of 2.7 µg/g and by formation of soluble calcium-carbonate-uranyl complexes in groundwater. Arsenic is more heterogeneously distributed in rock than U, with localized enrichment occurring near sulfide-mineral bearing ore deposits. While > 2000 µg/L As is observed present in chemically reduced groundwater, As attenuation is also observed through sorption onto Fe-(oxyhydr)oxides. Despite As-rich groundwater, surface-water As concentrations are consistently low (< 1 µg/L), likely due to As attenuation in groundwater discharge zones. This work provides understanding of processes controlling U and As at a regional scale and presents baseline against which possible water-quality changes induced by climate change or industrial activity can be evaluated.

1. Introduction

Uranium and arsenic contamination pose a concern for the protection of the environment and for water quality. Neither of these elements have any known biological function (Acharya and Apte, 2013; Plant et al., 2014). Arsenic is mutagenic, carcinogenic, and teratogenic; it is “unclear whether there is any safe dose to humans” (Plant et al., 2014). Uranium hazards are primarily linked to chemotoxicity (as opposed to radiation damage): elevated exposure to U can cause oxidative damage to biological tissues in fish and aquatic invertebrates, and kidney damage to humans (Goulet et al., 2011; Muscatello et al., 2020; Muscatello and Liber, 2009). In Canada, federal guidelines for the protection of aquatic life are 15 µg/L for U and 5 µg/L for As (Canadian Council Of Ministers Of the Environment, 1999a, 1999b).

Water contamination from U and As may arise through mobilization of geogenic sources of these elements during weathering processes (Pichler and Mozaffari, 2015; Smedley and Kinniburgh, 2002

). Most waters unaffected by anthropogenic activity contain µg/L or lower concentrations of U and As (Goulet et al., 2011; Smedley and Kinniburgh, 2002). However, groundwaters with U concentrations reaching hundreds to thousands of µg/L through geogenic mobilization have been reported in several localities worldwide, often in association with granitic or sedimentary geological environments (Asikainen and Kahlos, 1979; Gascoyne, 2004; Kim et al., 2004; Kurttio et al., 2002; Lee et al., 2001; Orloff et al., 2004; Post et al., 2017; Reszat and Hendry, 2007; Rosen et al., 2019; Smedley et al., 2006; Tixier and Beckie, 2001; Welch and Lico, 1998; Wu et al., 2014). Chronic exposure of humans to U sourced from crystalline-bedrock U-rich groundwater can lead to release of urinary indicators for kidney toxicity, although it is still unclear whether clinically significant kidney damage ensues (Kurttio et al., 2002; Zamora et al., 2010). Arsenic-rich natural groundwaters have also been documented, usually in association with either (1) regions of geologically young sediments with slow hydrogeological flow rates; (2) geothermal activ-

* Corresponding author at: Lorax Environmental Services Ltd., 2289 Burrard St, Vancouver V6J 3H9, Canada.

E-mail address: eskiersz@eoas.ubc.ca (E.K. Skierszkan)

ity; or (3) ore deposits where sulfide mineral oxidation occurs (Smedley and Kinniburgh, 2002).

The mobility of U and As in aqueous environments is generally controlled by pH, redox, and chemical interaction with ligands and mineral surfaces. Uranium(VI) and U(IV) are the two most common oxidation states of U; U(IV) being generally insoluble at $\text{pH} > 3$, while U(VI) forms the relatively soluble uranyl (UO_2^{2+}) aquocation (Cumberland et al., 2016). Uranium(VI) solubility is generally limited by sorption of UO_2^{2+} to mineral surfaces. However, U(VI) sorption is hindered by complexation of UO_2^{2+} with various ligands. In many groundwaters, U mobility is promoted by the formation of complexes $\text{Ca}_2\text{UO}_2(\text{CO}_3)_3$ and $\text{CaUO}_2(\text{CO}_3)_3^{2-}$ that inhibit uranyl sorption and U(VI) reduction (Stewart et al., 2011, 2010). In most aqueous environments, As forms the oxyanions arsenate [$\text{As}(\text{V})\text{O}_4^{3-}$] and arsenite [$\text{As}(\text{III})\text{O}_3^{3-}$], which are variably protonated depending on pH. Sorption to various mineral surfaces can attenuate aqueous As, and is dependent upon pH and competition with various other solutes (Dixit and Hering, 2003; Goldberg, 2002; Grafe et al., 2001; Helle et al., 2008).

At present there is generally little publicly available data on U and As distribution in subarctic regions due to their remoteness and low population density (Colombo et al., 2018; McClelland et al., 2008). Subarctic regions are seeing growing interest from the mining industry as remote mineral deposits become increasingly economically attractive. Mining may enhance mobilization of U and As relative to baseline conditions because mine wastes such as waste rock and tailings have high surface area that can be exposed to oxidative weathering environments, promoting chemical weathering of minerals to a greater degree than in the pre-mining environment (Blowes et al., 2014; Clark and Raven, 2004; Goulet et al., 2011; Lindsay et al., 2015). A key component in successful mine-waste management therefore lies in a detailed characterization of the baseline (pre-mining) environment, which provides a natural analogue to identify metal(loid) sources and mobilization patterns from the local geological units that may eventually enter the mine waste stream (Nordstrom, 2015). In addition, baseline characterization is required to develop local water-quality objectives, in particular in areas where elevated geogenic metal(loid) concentrations are naturally present. Besides mining activity, another possible perturbation to U and As mobilization in subarctic environments is the thaw of perennially frozen ground (permafrost), which leads to greater soil and bedrock chemical weathering, more active groundwater circulation, and greater microbial activity (Colombo et al., 2018; O'Donnell et al., 2012; Smith et al., 2007; Striegl et al., 2005; Toohy et al., 2016; Walvoord and Striegl, 2007). Given these possible perturbations, a detailed understanding on U and As sources and mobilization processes is required in subarctic regions.

This study presents a hydrogeochemical assessment of U and As in the Dawson Range, northwest Canada, a remote subarctic region where naturally elevated levels of these contaminants are present. The primary objective is to identify baseline U and As distribution in rock, sediment, and water, and to identify conditions that lead to their release in this region. Baseline assessment of U and As distribution has implications for water-quality management in subarctic regions at a pressing time when perturbations to natural hydrogeochemical cycles from thawing permafrost and industrial activity are anticipated.

2. Study site

The study area is located within the Dawson Range, a mountainous region lying near the Yukon-Alaska border (Fig. 1). This region is remote and sparsely populated and thus has seen relatively little anthropogenic impact to date. It lies within the traditional territory of several indigenous groups, including the Tr'ondëk Hwëch'in, White River, and Selkirk First Nations (Yukon Environment Geomatics, 2013).

Land uses include wild food gathering, trapping, outdoor recreation, and mineral exploration (Goldcorp, 2017).

Local elevations generally range between approximately 400 and 1400 m above sea level. The region was unglaciated during the Pleistocene (Duk-Rodkin, 1999) and has discontinuous permafrost coverage (Bond and Lipovsky, 2011). Regional bedrock is composed of metamorphic and granitic rocks (Wainwright et al., 2010; Ryan et al., 2013; Colpron et al., 2016). Dominant geological units include: (1) the Permian Sulphur Creek suite granitoids; (2) the Permian Klondike assemblage metavolcanics (the extrusive equivalent of the Sulphur Creek suite); (3) the Devonian Snowcap assemblage metasiliciclastics; and (4) Whitehorse suite granitic rocks, produced by largescale Cretaceous intrusions. North of the Yukon River, a major fault separates these units from the Mississippian Simpson Range suite granitoids (Colpron et al., 2016).

Several mineral deposits are present in Dawson Range (Fig. 1) and mining claims cover close to half of the area featured in this study (Fig. S2). The two most advanced mineral-exploration ventures are Coffee Mine Project (CMP, owned by Newmont, Fig. S3) and the Casino Mine Project (owned by the Casino Mining Corp., Fig. S4), which have submitted proposals for open-pit mining to the Yukon Environmental and Socio-Economic Assessment Board (Casino Mining Corp., 2014; Goldcorp, 2017) (Fig. 1). The Coffee deposit is a structurally controlled gold deposit where auriferous pyrite, arsenian pyrite, and arsenopyrite were produced during hydrothermal alteration that followed the Cretaceous Whitehorse suite intrusion into Permian gneisses and schists (MacWilliam, 2018). The Casino deposit is a Cu-Au-Mo porphyry (Selby and Nesbitt, 2000). Both properties have substantial faulting and extensively weathered rocks that are locally classified in part based on their degree of oxidation. The Casino deposit generally has a higher sulfide mineral content and a lower carbonate mineral content than the Coffee deposit.

3. Methods

3.1. Data sources and processing

A regional geochemical database was produced by combining available rock, sediment, groundwater, and surface water geochemical analyses in the Dawson Range from pre-existing government and industry datasets. The resulting database comprises geochemical analyses of 1075 rock samples, 365 sediment samples, 3189 surface-water samples (from 547 sampling sites), and 384 groundwater samples (from 46 monitoring wells) (Table 1). Rock geochemical data from the Geological Survey of Canada (GSC Open File 8500) are generally representative of regional lithologies (Ryan et al., 2018), while samples from exploration drill-core at the Coffee and Casino mine projects are overprinted by ore deposits. Groundwater monitoring is focussed around the Coffee and Casino mine projects; however, as neither of these projects have begun active mining operations at present, groundwater chemistry represents baseline conditions. Monitoring wells at both properties are distributed between a few hundred meters to several kilometers from the ore-bearing zones. Surface-water samples includes regular (e.g., monthly to quarterly) sampling at select locations conducted by Coffee and Casino mine projects, and synoptic samples collected by the Canadian government as part of Regional Geochemical Survey (RGS) (Héon, 2003). We conducted an additional synoptic surface-water sampling round in the summer of 2019 in Dawson Range watersheds not routinely sampled by the Coffee and Casino mine projects. Sediment samples were collected during the RGS with coverage of most major creeks in the Dawson Range.

Uranium and As abundances in the various media were mostly determined by inductively-coupled-plasma mass spectrometry (ICP-MS), with a smaller number of U analyses by instrumental neutron activation analysis (INAA) and laser-induced fluorimetry (details of analyti-

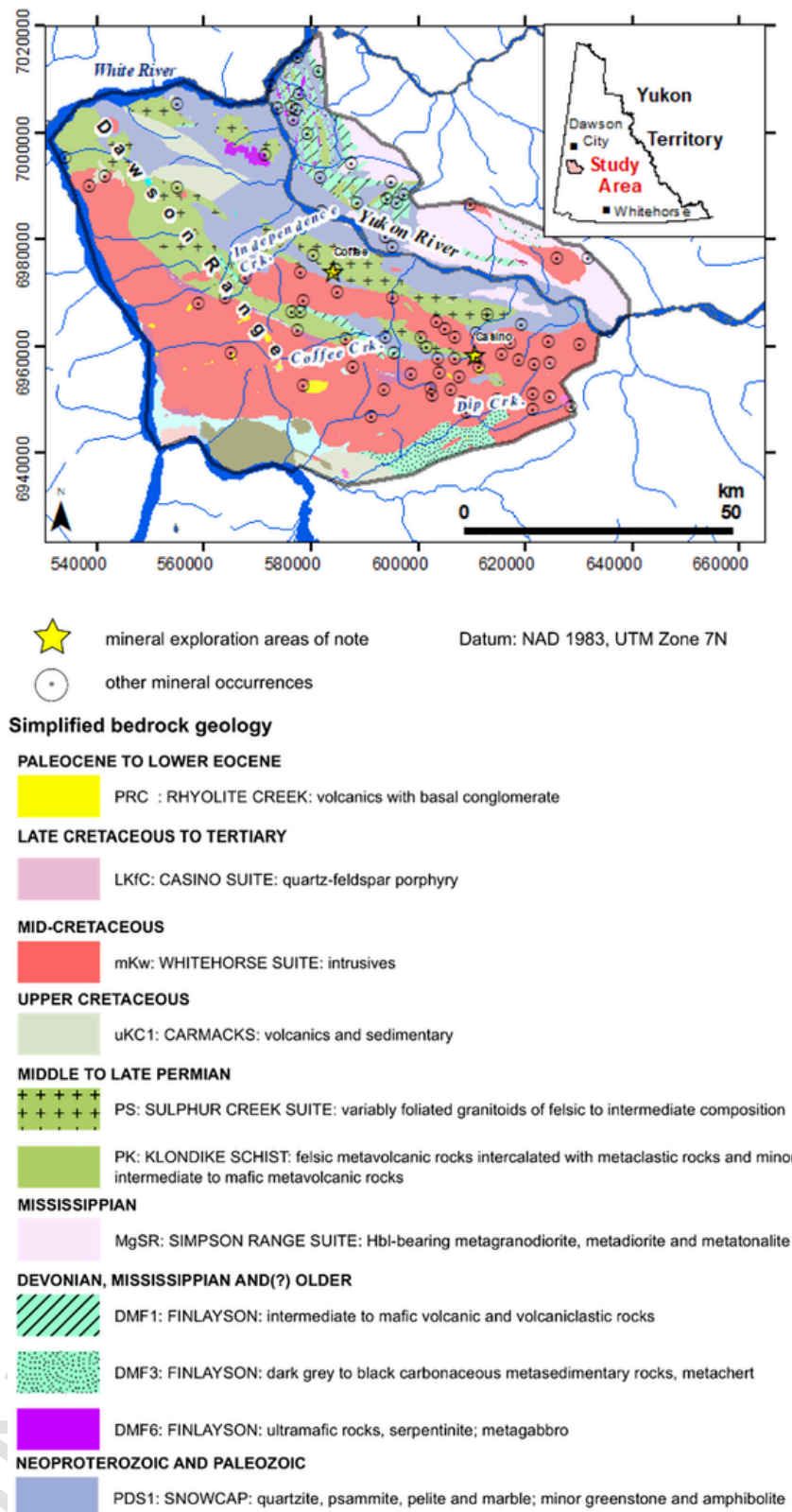


Fig. 1. Study site geological map with select mineral exploration projects and mineral occurrences identified by the Yukon Geological Survey. The inset map shows the study area location with Yukon, Canada. Data are from Geomatics Yukon (<ftp://ftp.geomaticsyukon.ca/GeoYukon/>). See also Fig. S2 for mining claims in the region. The legend only includes a subset of simplified geological units.

cal protocols in Supporting Information Section S.1). Each government and industry projects developed their own protocols to monitor trace-element analytical precision and accuracy, which generally included

blind field duplicate and filtered and preserved field-blank analyses and analyses of matrix spikes or certified reference materials (Supporting Information Section S.1). For the new surface-water samples col-

Table 1
Overview of geochemical data compiled for use in this study.

	Sample count	Sample count within study area	number of locations	Notes
Rock geochemistry				
GSC Open File 8500	811	151		GSC = Geological Survey of Canada
Coffee Mine Project (CMP)	460	460		
Casino	464	464		
Sediment geochemistry				
RGS Re-analysis 2016	20,411	365		RGS = Regional Geochemical Survey (Yukon Geological Survey, 2016)
Surface-water geochemistry				
RGS 2003	28,721	457	453	Only U, no As data (Héon, 2003)
Casino baseline	525	525	31	38 locations, data from 2008 to 2014
CMP baseline	2358	2185	41	43 locations, data from 2010 to 2018
New samples (this study)	22	22	22	22 locations, data from 2019
Groundwater geochemistry				
Casino baseline	169	169	28	28 monitoring wells, data from 1994 to 2014
CMP baseline	215	215	18	18 monitoring wells, from 2014 to 2018

lected as part of this study, U and As matrix-spike recoveries were $100 \pm 10\%$; duplicate U and As concentration measurements were equal within 3%, and field-filtered and acidified blanks contained $< 0.02 \mu\text{g/L}$ As and $< 0.002 \mu\text{g/L}$ U.

A water-quality database was constructed by compiling water-sample analyses from the various data sources. All replicate sample analyses were removed and values that were below reported detection limits (RDL) were converted to half of the RDL. All groundwater analyses with $> 5\%$ charge-balance error as determined using the geochemical calculation program PHREEQC (Parkhurst and Appelo, 2013) were discarded. This screening was not possible in surface-water samples because only a subset of major ions were analyzed during the RGS, precluding charge-balance calculations. Spatial determination of areas of U and As enrichment in surface water and sediment chemistry were identified through interpolation using ordinary spherical kriging with Ar-

Table 2
Summary statistics of U and As content in Dawson Range rocks.

Dataset	U ($\mu\text{g/g}$)				As ($\mu\text{g/g}$)					
	Min	Max	Median	Mean \pm 2 SD	n	Min	Max	Median	Mean \pm 2 SD	n
	Average upper continental crust ^a = 2.7 $\mu\text{g/g}$					Average upper continental crust ^{**} = 4.8 $\mu\text{g/g}$				
Open File 8500	0.01	19	2.1	3 \pm 5	651	0.3	1236	1.5	5 \pm 112	485
Coffee	0.2	53	3.5	6 \pm 12	459	1.4	7940	38	350 \pm 1730	457
Casino	0.2	75	3.7	4 \pm 9	464	0.3	389	8.0	16 \pm 60	464

^a Upper continental crust estimate from Rudnick and Gao (2014).

cMap software (version 10.6, ESRI, Redlands CA). Because surface-water concentrations display large temporal variations due to seasonal effects (e.g., snowmelt, rainfall events), maximum U and As concentrations at each sampling location were used as input in the kriging computation, as the focus is to identify zones of elevated concentrations. Mineral saturation indices (SI) and aqueous U speciation of groundwater analyses were computed in PHREEQC using the wateq4f.dat database, to which we added association constants for the species $\text{Ca}_2\text{UO}_2(\text{CO}_3)_3$ and $\text{CaUO}_2(\text{CO}_3)_3^{2-}$ of Dong and Brooks (2006). Mineralogy of drill-core samples from the CMP, representing mineralized and unmineralized granite, schist and, gneiss, was determined by powder X-ray diffraction with Rietveld Refinement. In a subset of samples, solid-phases were further characterized with Quantitative Evaluation of Materials by Scanning Electron Microscopy (QEMSCAN) (SGS Minerals, Vancouver, Canada).

4. Results and discussion

4.1. Geological occurrence of U

Bedrock in the Dawson Range generally has U content near the average upper crustal abundance (AUC) value of 2.7 $\mu\text{g/g}$ (Rudnick and Gao, 2014). Regional lithologies sampled by the GSC, generally unaffected by ore emplacement, have a median U content of 2.1 $\mu\text{g/g}$ with a maximum of 19 $\mu\text{g/g}$ (Table 2). However, among these samples, felsic and intermediate rocks have higher U content than their mafic counterparts (Fig. S5), consistent with the incompatible behavior of U during magmatic crystallization (Kyser, 2014). Four geologic units present in the region have median U contents above the average upper crust: the Rhyolite Creek complex; Casino suite; Whitehorse suite; and Sulphur Creek suite (Fig. S6), all of which are predominantly composed of felsic to intermediate igneous rocks or igneous protoliths. Magmatic U enrichment in local rocks is further evidenced by positive relationships of U abundance and ratios of Zr/TiO_2 and $(\text{Na} + \text{K})/\text{Al}$ (Fig. 2), which serve as indicators of incompatible element (e.g., U) enrichment in melts, and silicate-chain polymerization, respectively (Kyser, 2014). Uranium contents in rocks are higher in drill-core samples from the CMP and the Casino site than in GSC samples: the Coffee and Casino datasets show median concentrations of 3.5 and 3.7 $\mu\text{g/g}$, respectively, and maxima of 53 and 75 $\mu\text{g/g}$, respectively (Fig. S6 and Table 2).

4.2. Processes driving U enrichment in surface water and groundwater

Uranium contents in rocks outside of ore deposits are similar to, or moderately enriched relative to the AUC, yet dissolved U is observed at anomalously high concentrations in creeks throughout the Dawson Range (Fig. 3). 8% of the 547 surface-water sampling locations have median U concentrations are above the CCME aquatic life guideline (15 $\mu\text{g/L}$). The median, 5th percentile, and 95th percentile U concentrations in surface water are 2.2, 0.02, and 33 $\mu\text{g/L}$, respectively ($n = 2539$ analyses) (Fig. 4). These concentrations are anomalous when compared to typical surface-water U concentrations mea-

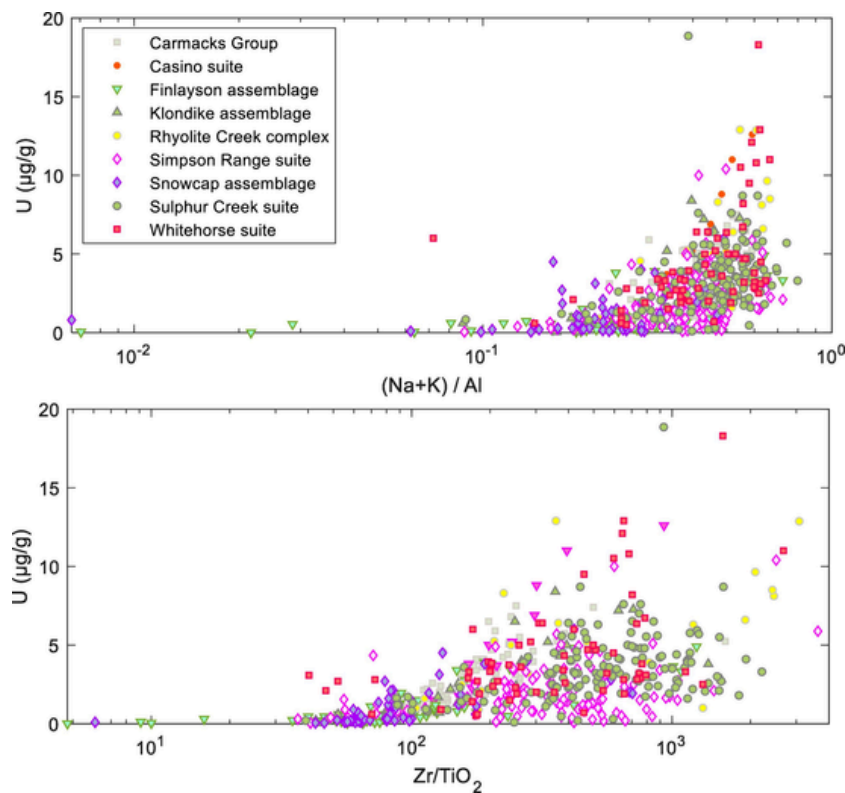


Fig. 2. Enrichment of U through magmatic processes in Dawson Range rocks, as seen through positive correlation with Zr/TiO_2 and $(Na + K)/Al$. Whole-rock data from GSC Open File 8500.

sured elsewhere. For example, 0.4% of the 28,721 water samples analyzed for U across Yukon in the RGS have U concentrations exceeding the CCME guideline. A survey of tens of thousands of U analyses in Canadian lakes and streams shows median concentrations commonly below $0.05 \mu\text{g/L}$ and not exceeding $0.06 \mu\text{g/L}$ (Goulet et al., 2011), and the median and maximum U concentrations in baseline surface waters in Europe are $0.89 \mu\text{g/L}$ and $21 \mu\text{g/L}$, respectively (Salminen et al., 2006).

Surface water U enrichment generally follows a NW-SE trend along the Yukon River, which is echoed in regional sediment geochemical data (Fig. 3). This enrichment overlaps spatially with exposures of Sulphur Creek gneiss and schist, Snowcap assemblage metasiliciclastics, Whitehorse suite intrusives, and Simpson Range granitoids. In this NW-SE trending region, interpolated U concentrations are regionally above the CCME guideline. However, lower U concentrations are present towards the western margin of the study area, which is also underlain by Whitehorse suite intrusives. The western portion of the Whitehorse batholith is granodioritic in composition, while the area closer to the Yukon river, locally known as the Coffee Creek phase, is more granitic and also known to have higher U content—consistent with greater U enrichment through magmatic differentiation (Colpron et al., 2016; MacWilliam, 2018). A noteworthy area of elevated U in surface water and sediments is present north of the Yukon river and near the eastern margin of the study area, where creeks commonly contain $>100 \mu\text{g/L}$ U (Fig. 3). Several bedrock samples in these drainages contain $>10 \mu\text{g/g}$ U and are field-logged by the GSC as monzogranite or syenogranite (Fig. 3). These rocks form through cooling of chemically evolved magmas that are enriched in incompatible elements such as U. Uranium enrichment in surface water and sediment therefore at least partially reflects the magmatically differentiated bedrock geology of the Dawson Range.

Uranium concentrations in surface water show associations with the parameters alkalinity, electrical conductivity (EC), dissolved Ca, dis-

solved sulfate, and pH. These associations are conveyed in Fig. 5 which shows the proportion of surface-water samples having U concentrations above the CCME aquatic life guideline calculated over a range in concentrations of these parameters (alkalinity EC, Ca, sulfate, pH), similar to the method proposed by Riedel and Kübeck (2018) for large datasets. When surface-water alkalinity is above 80 mg/L (as CaCO_3) and dissolved Ca is above 99 mg/L , $>80\%$ of samples exceed the CCME aquatic life guideline. High U concentrations also correlate with waters bearing electrical conductivity $>400 \mu\text{S/cm}$, sulfate $>349 \text{ mg/L}$, and $\text{pH} > 8$ (Fig. 5). These relationships generally indicate U enrichment in more mineralized surface waters, which are likely driven by a strong groundwater-discharge signature.

This hypothesis is further substantiated by the strong seasonality in U concentrations observed in U-rich surface-water monitoring locations. Peak concentrations occur during baseflow conditions, from November to May, and minima coincide with the higher flows of summer months (Fig. 6). Detailed concentration-flow and time-series plots show that concentrations of U, alkalinity, sulfate, and EC are substantially higher during winter baseflow, while peak DOC concentrations occur during high-flow summer conditions (Fig. 6). Peak U concentrations in surface water also correlate with elevated EC/DOC (Fig. S7). These relationships point to discharge of U-rich mineralized groundwater as the vector responsible for transfer of bedrock-derived U to surface water in the Dawson Range, while shallower interflow through organic-rich soils produces DOC-rich and U-poor surface water concentrations during periods of higher flow. Indeed, the median U concentration in groundwater is $17 \mu\text{g/L}$ ($n = 384$ analyses), respectively, with 40% of monitoring wells having median U concentrations above the $15 \mu\text{g/L}$ CCME guideline.

The high mobility of U in groundwater is associated with the dominance of calcium-carbonato-uranyl aqueous complexes (Stewart, 2008). Speciation calculations in PHREEQC show that these complexes comprise on average 93% of aqueous U in groundwater across all mon-

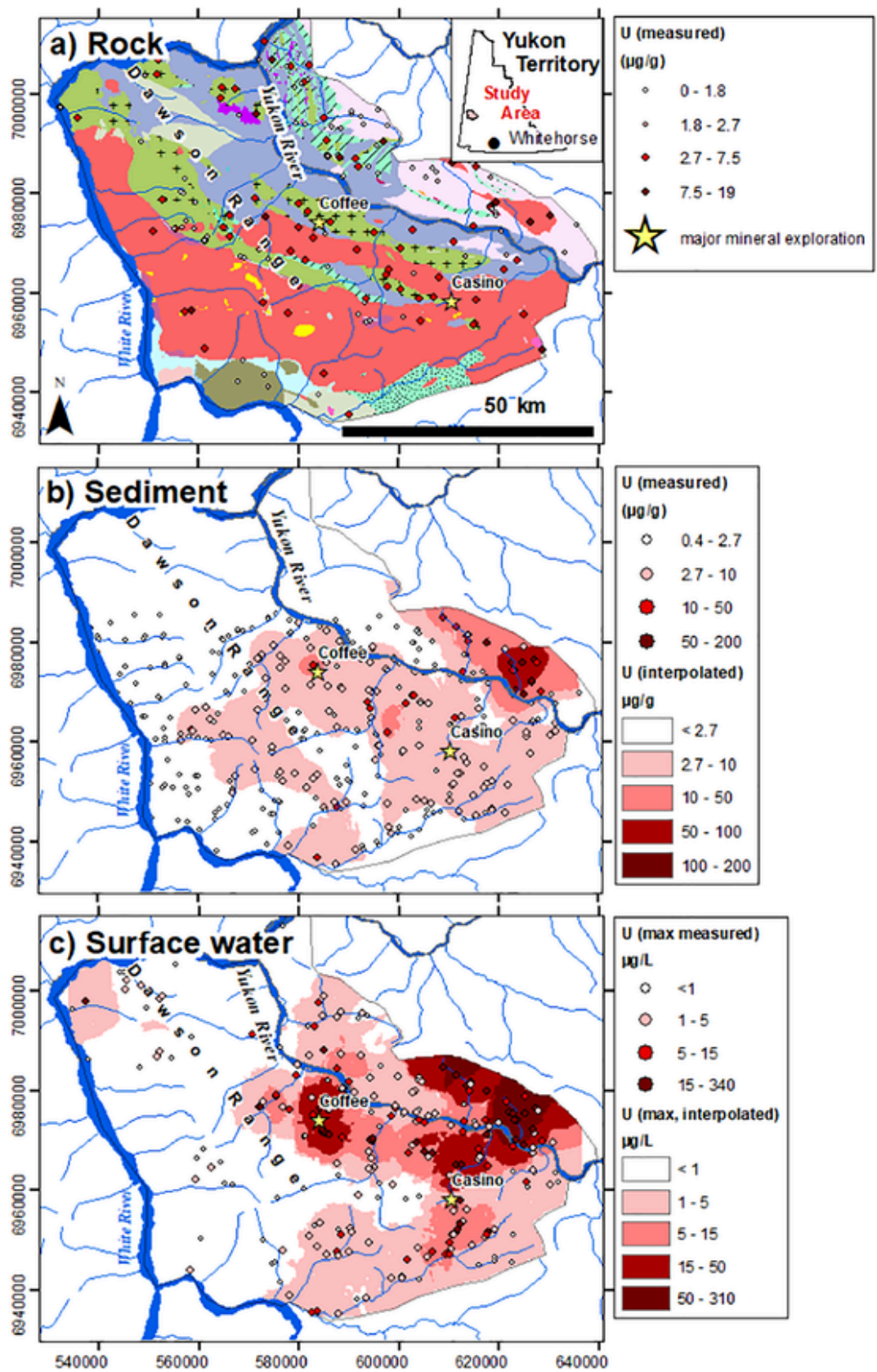


Fig. 3. Spatial distribution of U in rock (panel a, underlain by bedrock geological map), sediment (panel b), and surface water (panel c). Geographical coordinates are in UTM Zone 7N, NAD83 datum.

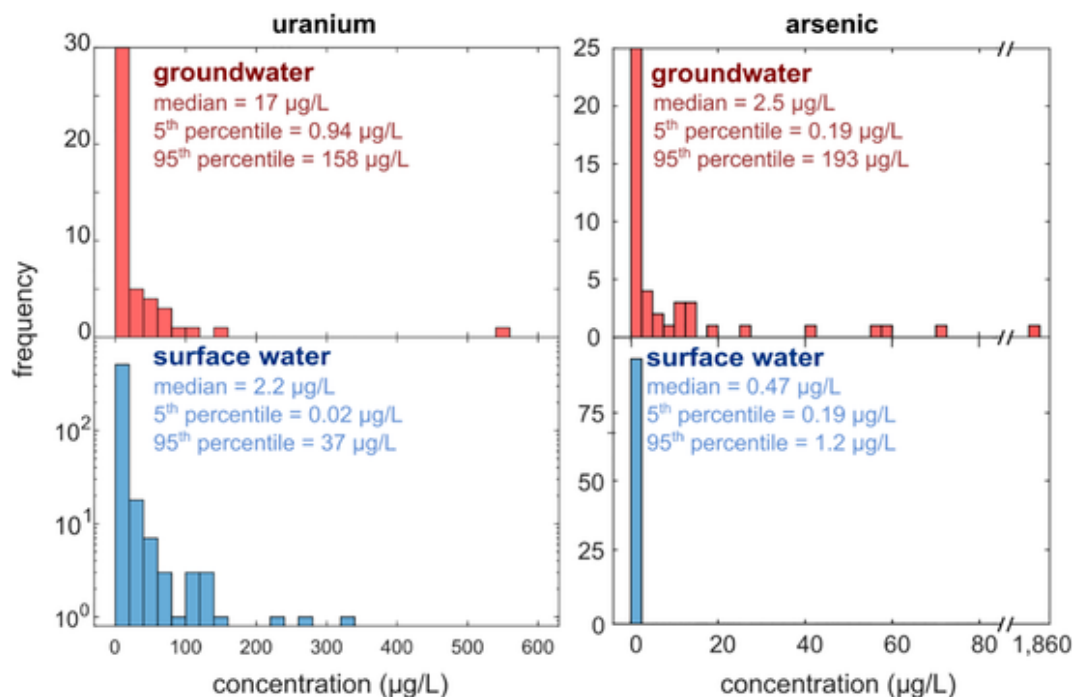


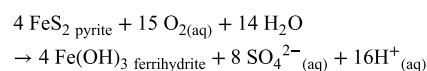
Fig. 4. Histogram showing the distribution of *median* groundwater U and As concentrations calculated at each monitoring well (above) and at each surface-water monitoring location (below). Medians are calculated for each sampling location to account for uneven sampling frequency between locations. Summary statistics are shown for the entire surface water and groundwater datasets.

itoring wells. Carbonato-uranyl complexes sorb poorly and resist U(VI) reduction, thus inhibiting the main geochemical reactions responsible for U attenuation in groundwater (Belli et al., 2015; Stewart et al., 2011, 2010). At the Coffee deposit, groundwater contains a median U concentration of 42 µg/L ($n = 215$ analyses), with the most elevated concentrations found in monitoring wells drilled in aquifers dominated by gneiss and schist (Fig. S8). These rocks contain several wt% carbonates, including calcite, dolomite, ankerite, and siderite (Table S2), the dissolution of which provides alkalinity and Ca available for U complexation. Excluding shallow active-layer zone monitoring wells (MW15-02AZ, MW15-03AZ, and MW15-05AZ; locations shown in Fig. S3), groundwater in monitoring wells located in gneiss and schist aquifers is close to calcite saturation (median SI from -0.5 to $+0.3$) and contains elevated Ca concentrations with medians at each well ranging from 43 to 255 mg/L. In contrast, lower dissolved U concentrations at the Coffee deposit are found in samples collected from monitoring wells drilled in granite, which contains <1 wt% carbonate minerals, resulting in lower groundwater Ca concentrations (medians at each well ranging from 22 to 47 mg/L), lower alkalinity, and undersaturation with respect to calcite (median SI at each well ranging from -1.4 to -0.3). (Fig. S9). Similarly, the absence of carbonate-bearing gneiss and schist and the lower carbonate content of the Casino deposit may in part explain its lower groundwater U concentrations, which have a median of 6.9 µg/L ($n = 169$ analyses). Additionally, monitoring wells at the Casino deposit with median U <1 µg/L are limited to four locations that also have <30 mg/L Ca and a significantly larger proportion of more U aqueous species that can adsorb such as $\text{UO}_2(\text{CO}_3)_2^{2-}$, UO_2^{2+} , and UO_2OH^+ (Kobayashi et al., 2020), at the expense of less-reactive calcium-carbonato-uranyl species (Fig. S9). The relationship between carbonate-bearing metamorphic rocks, Ca and alkalinity release, and elevated groundwater U concentrations in bedrock with similar solid-phase U abundances suggests that geogenic U mobilization is more strongly controlled by rock carbonate content than by solid-phase U abundance alone.

A key nuance regarding U mobility in groundwater is the sensitivity of U sorption to pH, $p\text{CO}_2$, and Ca concentrations. These relationships are conceptually illustrated by PHREEQC simulations of U sorption onto hydrous ferric oxide (HFO) (Fig. 7). Under atmospheric $p\text{CO}_2$ and in the absence of aqueous Ca, the U-HFO sorption envelope covers a broad range in pH from pH 4 to pH ~ 8.5 . However, at higher $p\text{CO}_2$ of $10^{-1.5}$ atm—a level frequently attained in Dawson Range groundwater—the span of the sorption envelope dramatically narrows to pH 4 to pH ~ 6.5 . For $p\text{CO}_2 \geq 10^{-3.5}$ atm, input of 25 mg/L Ca, which is on the lower end of observed groundwater Ca concentrations (median = 56 mg/L, $n = 384$ analyses), further narrows the U sorption envelope. This sensitivity of U sorption to variations in $p\text{CO}_2$ and Ca has been confirmed experimentally (Fox et al., 2006; Kobayashi et al., 2020; Mahoney et al., 2009; Stewart et al., 2010; Waite et al., 1994). As these $p\text{CO}_2$, pH, and dissolved Ca variations are easily within the range of values in Dawson Range groundwater, they can exert a large control on dissolved U concentrations.

One question that requires further investigation is whether regional U mobilization is affected by the presence of ore deposits. One possibility is that hydrothermal fluids related to ore genesis have re-mobilized U and pre-concentrated it into fractures at higher levels than those found in the country rock. Such fracture zones could be more prone to weathering as they act as preferential groundwater flowpaths. Alternatively, formation of calcium-carbonato-uranyl complexes may be indirectly promoted and solubilize U after sulfide-mineral oxidation in the presence of (excess) carbonate minerals. Sulfide-mineral oxidation produces sulfuric acid, which leads to carbonate mineral dissolution and Ca and bicarbonate release as per the sequence of geochemical reactions below:

- (i) pyrite oxidation releases sulfuric acid



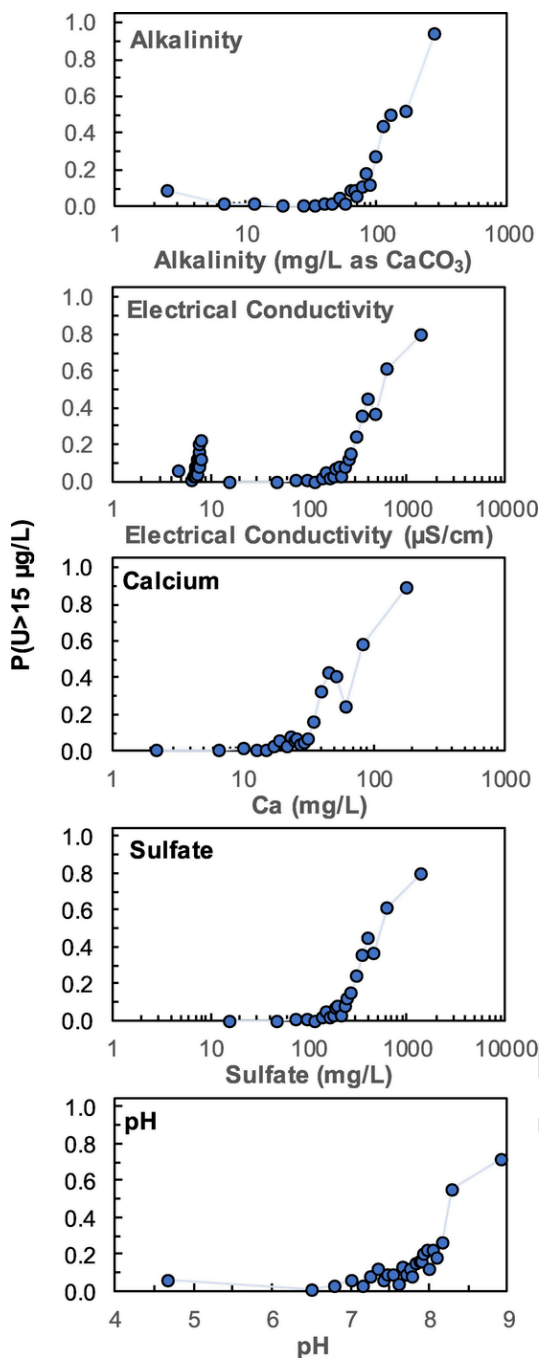
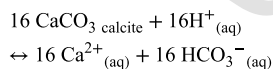
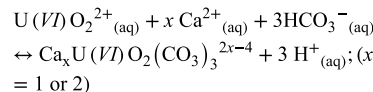


Fig. 5. Proportion of surface-water samples having U concentrations above the CCME guideline value (15 µg/L) that was calculated over different ranges in alkalinity, electrical conductivity, calcium, sulfate, and pH. For example, when surface-water alkalinity is above 170 mg/L as (CaCO₃), 94% of samples have U > 15 µg/L.

(ii) calcite (excess present) dissolution buffers H⁺ and liberates alkalinity and Ca.



Following these reactions, alkalinity and Ca released from calcite dissolution can form mobile aqueous complexes with U(VI):



These reactions could favor U desorption so long as there is a stoichiometric excess of calcite over sulfide and pH remains buffered. This hypothesis is supported by the observation that the most U-rich groundwater around the Casino property is frequently encountered in wells installed directly proximal to the ore deposit (i.e., wells HG10-01, HG10-02, HG10-05 and MW13-01D), where aqueous geochemistry reflects a strong sulfide-mineral oxidation signature (hundreds of mg/L SO₄²⁻) under well-buffered conditions (pH ≥ 6.7 and alkalinity ≥ 127 mg/L as CaCO₃) (Figs. S4 and S7). It may also account for the high probability of U concentrations above the CCME guideline value of 15 µg/L in surface waters where elevated dissolved sulfate (> 349 mg/L) is present (Fig. 5). Although more detailed experimental work should be conducted to test this hypothesis, the possibility of enhanced U release in association with chemical reactions that are inherent to sulfide-mineral deposits has implications for U release during weathering of mine wastes under neutral-rock drainage conditions (NRD), where chemical weathering rates are usually higher than in pre-mining rock. Additionally, promotion of U release near ore deposits could bear ramifications for mineral exploration in crystalline bedrock terranes as dissolved U and sulfate anomalies may reflect ore deposit weathering.

4.3. Association of As with ore deposits

In opposition to the regional geological enrichment of U, the distribution of As in Dawson Range rocks is more heterogeneous and is controlled by localized weathering of ore deposits. The geochemical fingerprints of the Coffee and the Casino deposits are visible through high As content in sediment in their vicinity (Fig. 8). Geochemical analyses show that As contents in rock frequently reach thousands of µg/g at Coffee (median 38 µg/g, maximum 7940 µg/g), and tens of µg/g at Casino (median 8.0 µg/g, maximum 389 µg/g) (Fig. 10). These As contents are well above the AUC value of 4.8 µg/g (Table 2). In contrast, rock samples collected by the GSC and generally outside of these ore deposits have substantially lower As contents, with a median of 1.5 µg/g (Fig. 8 and Table 2). Standard-deviation (SD) values on the mean As contents of all three rock-sample datasets (Coffee, Casino and the GSC Open File 8500) are all one to three orders of magnitude above the SDs of the corresponding U contents, reflecting the higher heterogeneity of As content in rocks (Table 2). This spatial distribution and heterogeneity can be directly explained by the presence of As-bearing minerals including scorodite, arsenopyrite, and arsenian pyrite that are observed by XRD and QEMSCAN analyses of drill-core from the Coffee deposit (Table S1). Such associations are consistent with the chalcophile behavior of As and its common co-occurrence with gold mineralization (Blowes et al., 2014; Plant et al., 2014) (Fig. 9).

4.4. Controls on As mobilization in groundwater and surface water

Groundwater As concentrations scale directly with the rock As abundances of a given ore deposit. The Coffee deposit (As-rich rock) shows significantly higher As concentrations in groundwater than the Casino deposit (lower rock As) (p < 0.001, Mann-Wilcoxon Test), with a respective medians of 13 µg/L (n = 215 analyses) and 1.3 µg/L (n = 169 analyses), respectively. Although surface-water As concentrations are consistently low (median 0.47 µg/L), they occur at

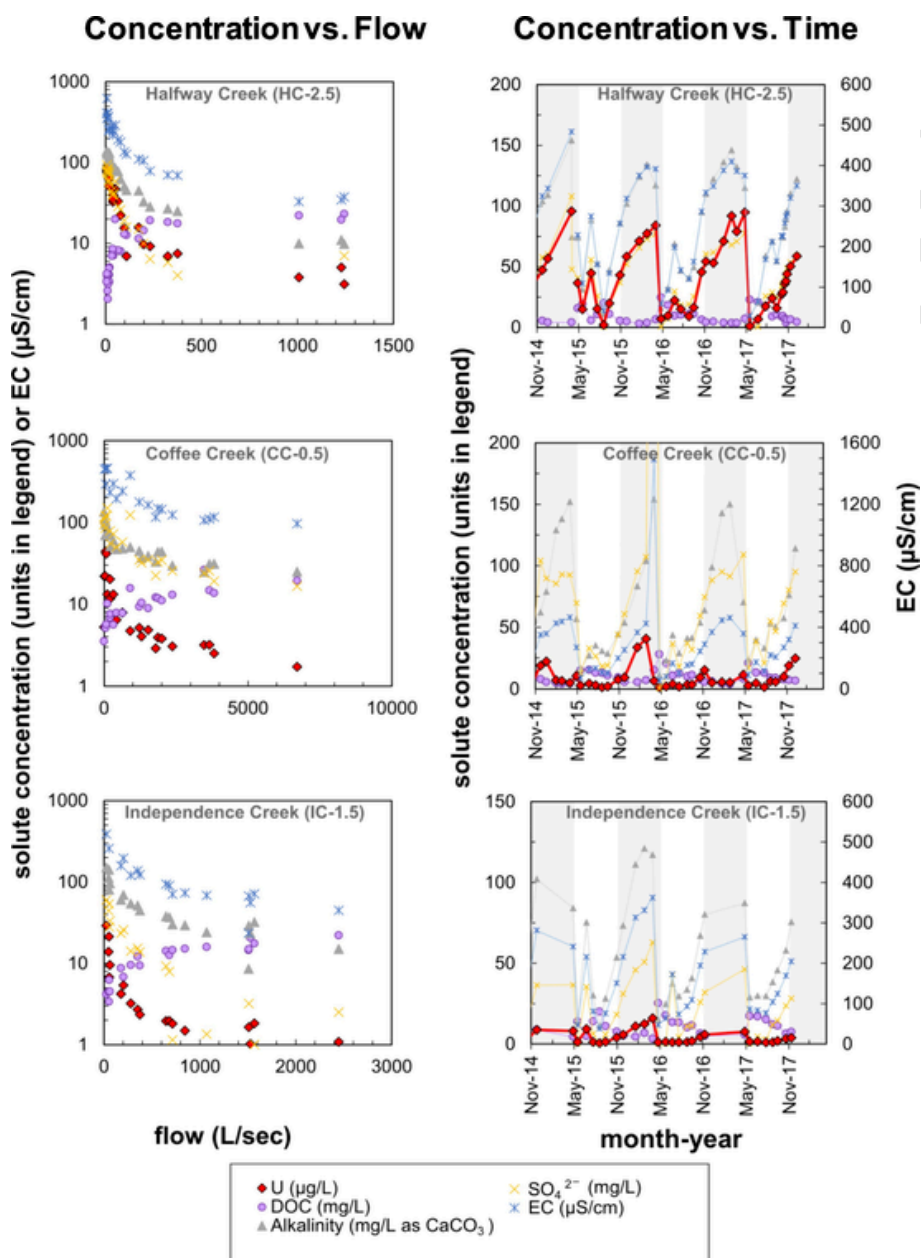


Fig. 6. Relationship between surface-water chemistry and flow (left side) and time of year (right side) at select surface-water hydrometric stations. Low-flow conditions, which occur between November and May (gray shading in right-side panel), coincide with peak U, alkalinity, sulfate, and electrical conductivity (EC), while summer peak flows coincide with lower concentrations of these parameters but more elevated DOC. Creek locations are shown in Fig. S3.

slightly higher concentrations around the Coffee deposit (Figs. 4 and 8). Higher dissolved As at the Coffee deposit may be further explained by considering the mineralogical characteristics of host rocks. For example, sorption onto Fe-(oxyhydr)oxides is a key control on As in oxidized orebodies (Clark and Raven, 2004; Desbarats et al., 2015; Paktunc and Bruggeman, 2010; Smedley and Kinniburgh, 2002; Vriens et al., 2019). QEMSCAN analyses confirm that the majority of solid-phase As in the oxidized portion of the Coffee deposit is indeed associated with Fe-oxides and Fe-(oxyhydr)oxides (Fig. S10). Both deposits also show relative As enrichment in their respective oxidized zones in comparison with their hypogene or sulfide-zone counterparts (Fig. 10). However, the Fe-(oxyhydr)oxide abundance is most likely lower at the Coffee deposit because it formed from a more sulfide-poor hydrothermal system than the Casino deposit, as evidenced by comparing the sulfide content in their respective unoxidized/hypogene

zones (Fig. 10). In addition, groundwater at the Coffee deposit has significantly higher alkalinity owing to the greater carbonate/sulfide mineral ratios and its carbonate = bearing gneiss and schist country rock (Fig. S11). Elevated alkalinity may further inhibit As sorption, either through direct competition of carbonate and arsenate or arsenite ions at the sorption surface, or formation of aqueous As-carbonate complexes (Arai et al., 2004; Brechbühl et al., 2012; Kim et al., 2000; Saalfeld and Bostick, 2010). Thus the Coffee deposit holds a combination of more As-rich rock, (presumably) lower sorption-site availability, and greater groundwater alkalinity, with all of these factors promoting higher groundwater As concentrations relative to the Casino deposit.

While oxidized zones show As attenuation via sorption to Fe-(oxyhydr)oxides, co-occurrence of elevated Fe(II) and As in groundwater suggests remobilization of As is occurring under reducing condi-

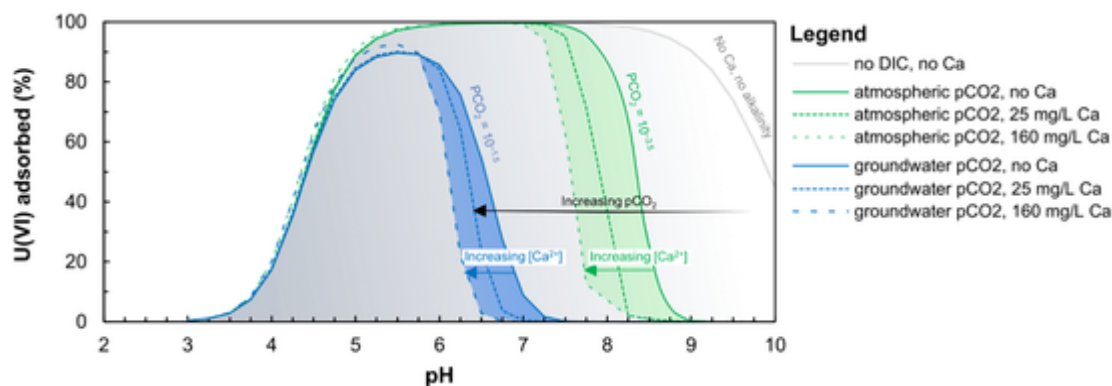


Fig. 7. Simulated U sorption behavior as a function of pH and $p\text{CO}_2$. Green lines are for water in equilibrium with atmospheric gas ($p\text{CO}_2 = 10^{-3.5}$ atm) and blue lines are for CO_2 -rich groundwaters typical of the Dawson Range ($p\text{CO}_2 = 10^{-1.5}$ atm). Because groundwaters usually have a pH between 6 and 8.5, U sorption behavior is strongly dependent on $p\text{CO}_2$ and the Ca concentration. Modeled U sorption behavior was conducted in PHREEQC for a water containing: 95 mg/L U, 26 mg/L Ca, 46 mg/L Na, 71 mg/L Cl, and weak hydrous ferric oxide sorption sites (HFO_wOH) having a concentration of 0.1 g/L, a surface area of 600 m^2/g , and a surface-site availability of 0.002 mol/L. Dissolved inorganic carbon (DIC) concentrations were fixed by $p\text{CO}_2$. The wateq4f.dat database was used, with the addition of association constants for $\text{Ca}_2\text{UO}_2(\text{CO}_3)$ and $\text{CaUO}_2(\text{CO}_3)^{2-}$ from Dong and Brooks (2006). (For interpretation of the references to color in this figure legend, the reader is referred to the web version of this article.)

tions (Fig. 10). Indeed, As-rich groundwaters at Coffee have $\text{Fe} > 100 \mu\text{g}/\text{L}$ (Fig. 10). Groundwater containing the highest As concentrations was collected from a well cluster (MW14-05A/B) screened in granite below a zone of gold mineralization where median As concentrations are 1860 $\mu\text{g}/\text{L}$ and 161 $\mu\text{g}/\text{L}$, respectively (Fig. S7). These groundwaters are also characterized by elevated dissolved Fe(II) and FeS saturation indices near zero (Fig. S7). Arsenic release after reductive dissolution or phase-transformation of Fe-(oxyhydroxides) under near-neutral pH conditions has been identified in many aquifers (Biswas et al., 2012; Harvey et al., 2002; Kelly et al., 2005; Larson et al., 2012; Plant et al., 2014; Puccia et al., 2015; Saalfield and Bostick, 2010; Sracek et al., 2004). A decrease in redox potential after the initial sulfide-mineral oxidation and As sorption processes is required to drive this As remobilization. Plausible drivers for a change in groundwater redox conditions include: (1) oxidation of dissolved organic matter, which is key factor in mobilizing As in groundwater globally (Biswas et al., 2012; Smedley and Kinniburgh, 2002); and/or (2) a rise in the water table occurring after the initial sulfide-mineral oxidation that would decrease influx of oxidants into the aquifer. Regardless of the mechanism involved, the occurrence of elevated As in Fe(II)-bearing groundwater indicates that oxidized mine wastes from the Dawson Range have the potential to leach As if stored under reducing conditions such as subaqueously.

Despite the presence of As-rich groundwater around ore deposits all surface water As concentrations in the study area are below the CCME guideline for the protection of aquatic life (Fig. 8). The lack of appreciable As transport into surface water suggests that As is being attenuated during discharge of groundwater to surface water, providing a contrast to the more conservative behavior of dissolved U. While no direct observations of As attenuation in groundwater discharge zones are available in this study, many other studies in regions of elevated groundwater As have documented that oxidation of Fe(II) during groundwater discharge leads to Fe(III)-(oxyhydr)oxide precipitation which can effectively capture dissolved As and maintain its concentrations $< 1 \mu\text{g}/\text{L}$ in oxic surface water (Ahmad et al., 2020; Datta et al., 2009; van Genuchten et al., 2020). We hypothesize that a similar mechanism is responsible for the limited As transfer from groundwater to surface water in the Dawson Range.

5. Summary and implications

This study shows regionally elevated baseline U in groundwater and surface water, and locally elevated As in groundwater in the Daw-

son Range, Yukon, Canada, a relatively undisturbed and remote subarctic region bearing several prospective mineral deposits. Regional U mobilization is driven by the occurrence of crystalline bedrock and carbonate-mineral dissolution that promotes mobility of $\text{U}_{(\text{aq})}$ as calcium-carbonate-uranyl complexes. Although U enrichment in Dawson Range rocks is only marginally enriched compared to average upper crustal abundance, $\text{U}_{(\text{aq})}$ mobility is sufficient to produce regional-scale groundwater and surface water U reaching hundreds of $\mu\text{g}/\text{L}$, i.e., an order of magnitude above the Canadian water-quality guidelines for the protection of aquatic life and for drinking water. It is plausible that U release is further promoted by weathering of sulfide-ore deposits, either by generation of Ca- and carbonate-rich water after sulfide-mineral oxidation and concomitant carbonate-mineral dissolution reactions, or via hydrothermal concentration of U into fractures around ore deposits that might act as preferential conduits for groundwater flow and chemical weathering.

In contrast to U, the distribution of geogenic As is more heterogeneous, with orders-of-magnitude differences in rock abundances that are strongly controlled by As-bearing sulfides and oxides associated with ore deposits. While dissolution of these phases under reducing conditions can produce As concentrations in groundwater in the mg/L range, sorption onto secondary Fe-oxides and Fe-(oxyhydr)oxides most likely mitigates its transport to surface water bodies. Arsenic transport is therefore less conservatively behaved than U.

As the Dawson Range hosts several prospective mining projects and is also underlain by discontinuous permafrost that is at risk of thawing as a result of global warming (Grosse et al., 2011), future environmental monitoring should be conducted to assess whether future changes in hydrological and geochemical processes might impact mobility of U and As in a subarctic region already enriched by these potentially hazardous elements.

CRedit authorship contribution statement

Elliott K. Skierszkan: Conceptualization, Methodology, Formal analysis, Investigation, Data curation, Writing - original draft, Writing - review & editing, Visualization, Funding acquisition. **John W. Dockrey:** Conceptualization, Investigation, Writing - original draft, Writing - review & editing, Funding acquisition, Supervision. **K. Ulrich Mayer:** Writing - original draft, Writing - review & editing, Supervision. **Roger D. Beckie:** Writing - original draft, Writing - review & editing, Supervision, Funding acquisition.

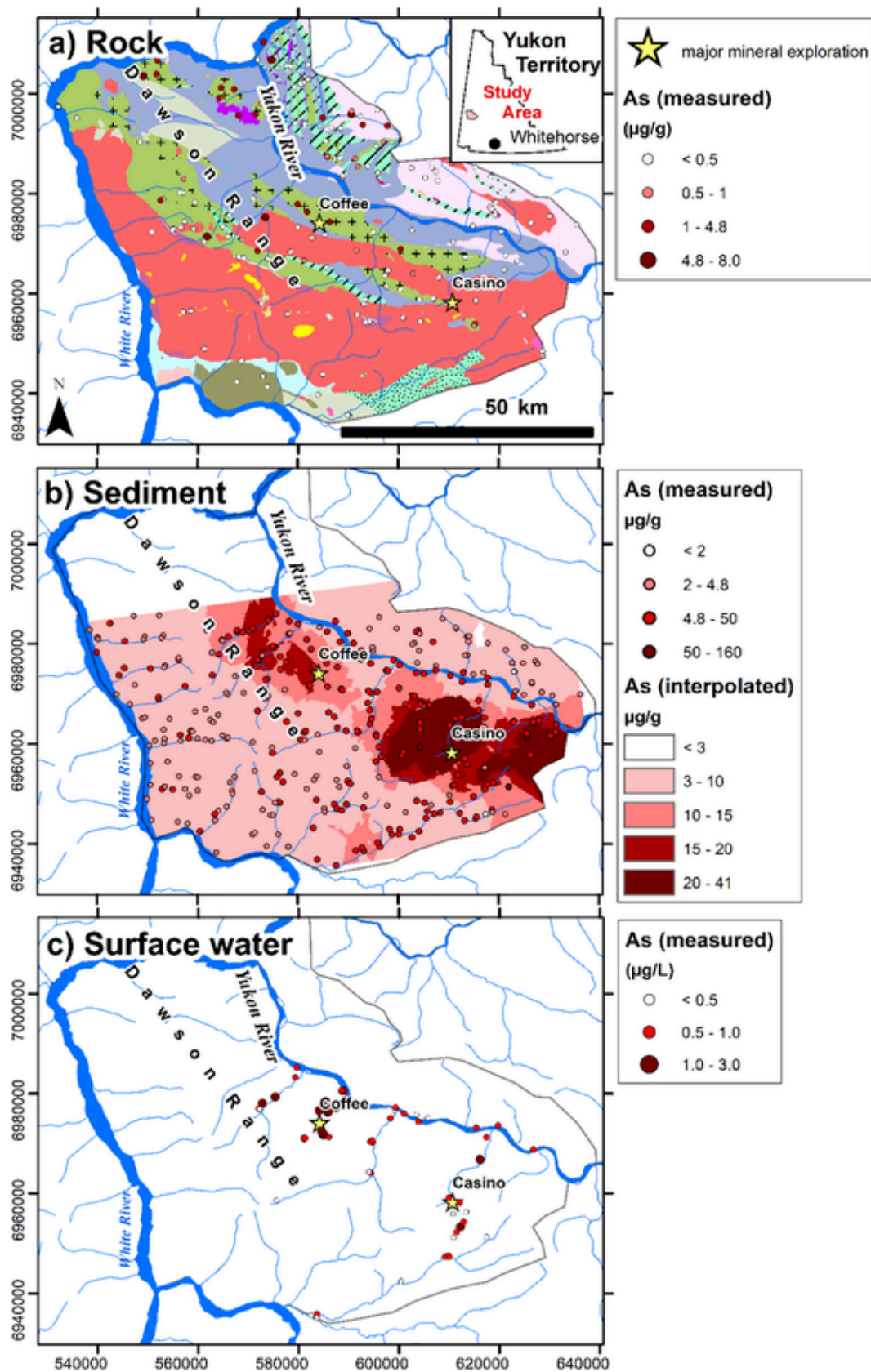


Fig. 8. Spatial distribution of As in rock (panel a underlain by bedrock geological map), sediment (panel b), and surface water (panel c). Geographical coordinates are in UTM Zone 7N, NAD83 datum. Note the absence of sediment samples in the northern part of the study area.

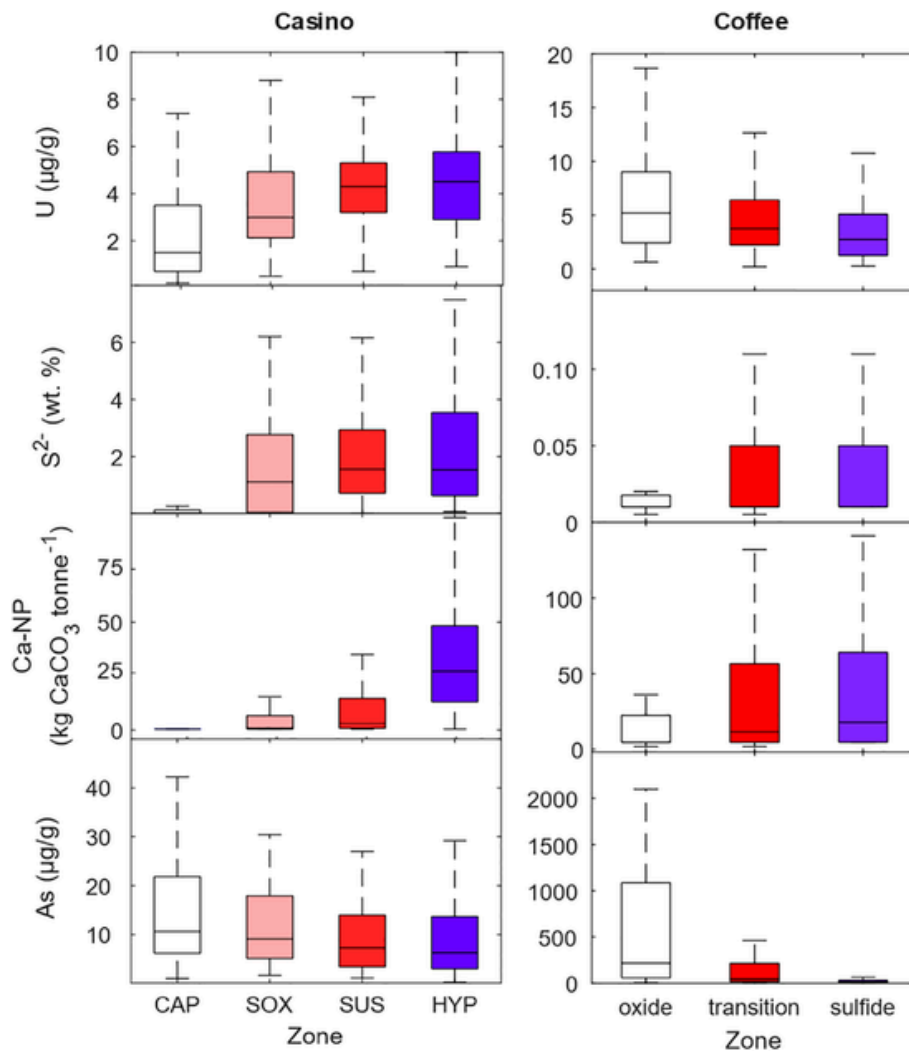


Fig. 9. Uranium, sulfide, carbonate neutralization potential (Ca-NP) and arsenic content in Casino and Coffee drill-core samples separated by locally defined geological weathering zones. At Casino: CAP = oxide cap, SOX = supergene oxide, SUS = supergene sulfide, HYP = hypogene; at Coffee: weathering zones are defined as “oxide”, “transition”, or “sulfide”. Note that y-axis scales are different between left and right panels.

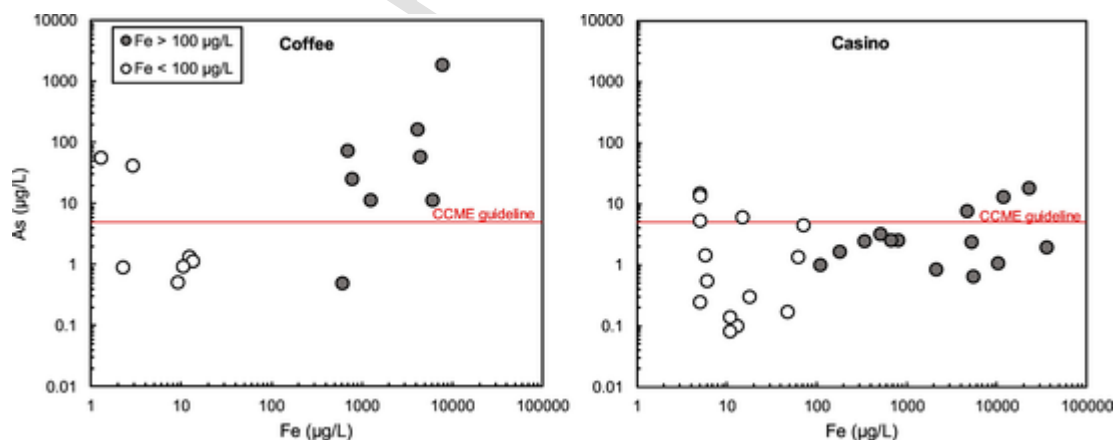


Fig. 10. Median dissolved As and Fe concentrations calculated at each groundwater well at Coffee (left) and Casino (right). Filled symbols are wells with median Fe concentrations above >100 $\mu\text{g/L}$.

Declaration of competing interest

The authors declare that they have no known competing financial interests or personal relationships that could have appeared to influence the work reported in this paper.

Acknowledgements

Funding was provided by Yukon Government (Water Resources Branch) through a Yukon Environmental and Socio-economic Assessment Board grant and by Mitacs through the Accelerate program. Newmont Corporation and the Casino Mining Corporation are thanked for generously providing geochemical data and facilitating access to field sampling sites. Research took place on the traditional territory of the Tr'ondëk Hwëch'in, White River, and Selkirk First Nations. The Tr'ondëk Hwëch'in First Nation is thanked for their contribution to fieldwork. Maurice Colpron is thanked for helpful conversations pertaining to Yukon geology.

Appendix A. Supplementary data

Supplementary data to this article can be found online at <https://doi.org/10.1016/j.jgexplo.2020.106607>.

References

- Acharya, C, Apte, S K, 2013. Insights into the interactions of cyanobacteria with uranium. *Photosynth. Res.* 118, 83–94. doi:10.1007/s11220-013-9928-9.
- Ahmad, A, Heijnen, L, de Waal, L, Battaglia-Brunet, F, Oorthuizen, W, Pieterse, B, Bhattacharya, P, van der Wal, A, 2020. Mobility and redox transformation of arsenic during treatment of artificially recharged groundwater for drinking water production. *Water Res.* 178, 115826. doi:10.1016/j.watres.2020.115826.
- Arai, Y, Sparks, D L, Davis, J A, 2004. Effects of dissolved carbonate on arsenate adsorption and surface speciation at the hematite - water interface. *Environ. Sci. Technol.* 38, 817–824.
- Asikainen, M, Kahlos, H, 1979. Anomalous high concentrations of uranium, radium and radon in water from drilled wells in the Helsinki region. *Geochim. Cosmochim. Acta* 43, 1681–1686. doi:10.1016/0016-7037(79)90187-X.
- Belli, K M, DiChristina, T J, Van Cappellen, P, Taillefert, M, 2015. Effects of aqueous uranyl speciation on the kinetics of microbial uranium reduction. *Geochim. Cosmochim. Acta* 157, 109–124. doi:10.1016/j.gca.2015.02.006.
- Biswas, A, Nath, B, Bhattacharya, P, Halder, D, Kundu, A K, Mandal, U, Mukherjee, A, Chatterjee, D, Mörth, C M, Jacks, G, 2012. Hydrogeochemical contrast between brown and grey sand aquifers in shallow depth of Bengal Basin: Consequences for sustainable drinking water supply. *Sci. Total Environ.* 431, 402–412. doi:10.1016/j.scitotenv.2012.05.031.
- Blowes, D W, Ptacek, C J, Jambor, J L, Weisener, C G, Paktunc, D, Gould, W D, Johnson, D B, 2014. The geochemistry of acid mine drainage. In: *Treatise on Geochemistry: Second Edition*, 2nd ed. Elsevier Ltd. doi:10.1016/B978-0-08-095975-7.00905-0.
- Bond, J D, Lipovsky, P S, 2011. Surficial geology, soils and permafrost of the northern Dawson Range. *Yukon Explor. Geol.* 2010, 19–32.
- Brechbühl, Y, Christl, I, Elzinga, E J, Kretzschmar, R, 2012. Competitive sorption of carbonate and arsenic to hematite: combined ATR-FTIR and batch experiments. *J. Colloid Interface Sci.* 377, 313–321. doi:10.1016/j.jcis.2012.03.025.
- Canadian Council Of Ministers Of The Environment, 1999. Canadian water quality guidelines for the protection of aquatic life – uranium. *Can. Environ. Qual. Guidel.*
- Canadian Council Of Ministers Of The Environment, 1999. Canadian water quality guidelines for the protection of aquatic life – arsenic. *Can. Environ. Qual. Guidel.*
- Casino Mining Corp Casino project – proposal for executive committee review. January 2014. Available through the Yukon Socio-economic Assessment Board at www.yesabregistry.ca2014 (Consulted September 10, 2018)
- Clark, I D, Raven, K G, 2004. Sources and circulation of water and arsenic in the Giant Mine, Yellowknife, NWT, Canada. *Isot. Environ. Health Stud.* 40, 115–128. doi:10.1080/10256010410001671014.
- Colombo, N, Salerno, F, Gruber, S, Freppaz, M, Williams, M, Fratianni, S, Giardino, M, 2018. Review: impacts of permafrost degradation on inorganic chemistry of surface fresh water. *Glob. Planet. Chang.* 162, 69–83. doi:10.1016/j.gloplacha.2017.11.017.
- Colpron, M., Israel, S., Murphy, D., Pigage, L., Moynihan, D., 2016. Yukon Bedrock Geology Map. Yukon Geological Survey, Open File 2016-1, 1:1,000,000 Scale Map and Legend.
- Cumberland, S A, Douglas, G, Grice, K, Moreau, J W, 2016. Uranium mobility in organic matter-rich sediments: A review of geological and geochemical processes. *Earth-Sci. Rev.* 159, 160–185. doi:10.1016/j.earscirev.2016.05.010.
- Datta, S, Mailloux, B, Jung, H B, Hoque, M A, Stute, M, Ahmed, K M, Zheng, Y, 2009. Redox trapping of arsenic during groundwater discharge in sediments from the Meghna riverbank in Bangladesh. *Proc. Natl. Acad. Sci. U. S. A.* 106, 16930–16935. doi:10.1073/pnas.0908168106.
- Desbarats, A J, Parsons, M B, Percival, J B, 2015. Arsenic mobility in mildly alkaline drainage from an orogenic lode gold deposit, Bralorne mine, British Columbia. *Appl. Geochem.* 57, 45–54. doi:10.1016/j.apgeochem.2014.11.015.
- Dixit, S, Hering, J G, 2003. Comparison of arsenic(V) and arsenic(III) sorption onto iron oxide minerals: Implications for arsenic mobility. *Environ. Sci. Technol.* 37, 4182–4189. doi:10.1021/es030309t.
- Dong, W, Brooks, S, 2006. Determination of the formation constants of ternary complexes of uranyl and carbonate with alkaline earth metals (Mg²⁺, Ca²⁺, Sr²⁺, and Ba²⁺) using anion exchange method. *Environ. Sci. Technol.* 40, 4689–4695. doi:10.1021/es0606327.
- Duk-Rodkin, A, 1999. Glacial limits map of Yukon Territory. In: *Geological Survey of Canada Open File 3694*.
- Fox, P M, Davis, J A, Zachara, J M, 2006. The effect of calcium on aqueous uranium(VI) speciation and adsorption to ferrihydrite and quartz. *Geochim. Cosmochim. Acta* 70, 1379–1387. doi:10.1016/j.gca.2005.11.027.
- Gascoyne, M, 2004. Hydrogeochemistry, groundwater ages and sources of salts in a granitic batholith on the Canadian Shield, southeastern Manitoba. *Appl. Geochem.* 19, 519–560. doi:10.1016/S0883-2927(03)00155-0.
- van Genuchten, C M, Behrends, T, Stipp, S L S, Dideriksen, K, 2020. Achieving arsenic concentrations of <1 µg/L by Fe(0) electrolysis: the exceptional performance of magnetite. *Water Res.* 168, 115170. doi:10.1016/j.watres.2019.115170.
- Goldberg, S, 2002. Competitive adsorption of arsenate and arsenite on oxides and clay minerals. *Soil Sci. Soc. Am. J.* 66, 413–421.
- Goldcorp The coffee gold mine – project proposal for executive committee screening. Pursuant to the Yukon Environmental and Socio-economic Act, March 2017 Available through the Yukon Environmental and Socio-economic Assessment Board at www.yesabregistry.ca2017
- Goulet, R R, Fortin, C, Spry, D J, 2011. Uranium. *Fish Physiol.* 31, 391–428. doi:10.1016/S1546-5098(11)31030-8.
- Grafe, M, Eick, M J, Grossl, P R, 2001. Adsorption of arsenate (V) and arsenite (III) on goethite in the presence of dissolved organic carbon. *Soil Sci. Soc. Am. J.* 1680–1687.
- Grosse, G, Romanovsky, V, Jorgenson, T, Walter, Ka, Brown, J, Overduin, P P, 2011. Vulnerability and feedbacks of permafrost to climate change. *EOS Trans. Am. Geophys. Union* 92, 73–80. doi:10.1002/ppp.689.
- Rowland, H F, Harvey, C F, Swartz, C H, Badruzzaman, A B M, Keon-Blute, N, Yu, W, Ali, M A, Jay, J, Beckie, R, Niedan, V, Brabander, D, Oates, P M, Ashfaq, K N, Islam, S, Hemond, H F, Ahmed, M F, 2002. Arsenic mobility and groundwater extraction in Bangladesh. *Science* (80-) 298, 1602–1606. doi:10.1126/science.1076978.
- Helle, U S, Postma, D, Jakobsen, R, Larsen, F, 2008. Sorption and desorption of arsenate and arsenite on calcite. *Geochim. Cosmochim. Acta* 72, 5871–5884. doi:10.1016/j.gca.2008.09.023.
- Héon, D (Compiler), 2003. Yukon Regional Geochemical Database - Stream Sediment Analyses. Yukon Geological Survey Database.
- Kelly, W R, Holm, T R, Wilson, S D, Roadcap, G S, 2005. Arsenic in glacial aquifers: sources and geochemical controls. *Ground Water* 43, 500–510. doi:10.1111/j.1745-6584.2005.0058.x.
- Kim, M, Nriagu, J, Haack, S, 2000. Carbonate ions and arsenic dissolution by groundwater. *Environ. Sci. Technol.* 34, 3094–3100. doi:10.1021/es990949p.
- Kim, Y S, Park, H S, Kim, J Y, Park, S K, Cho, B W, Sung, I H, Shin, D C, 2004. Health risk assessment for uranium in Korean groundwater. *J. Environ. Radioact.* 77, 77–85. doi:10.1016/j.jenvrad.2004.03.001.
- Kobayashi, Y, Fukushi, K, Kosugi, S, 2020. A robust model for prediction of U(VI) adsorption onto ferrihydrite consistent with spectroscopic observations. *Environ. Sci. Technol.* 54, 2304–2313. doi:10.1021/acs.est.9b06556.
- Kurttila, P, Päivi, A, Salonen, L, Saha, H, Pekkanen, J, Vaisanen, S B, Penttilä, I M, Komulainen, H, Päivi, K, Kurttila, A, Salonen, L, Saha, H, Pekkanen, J, 2002. Renal effects of uranium in drinking water. *Environ. Health Perspect.* 110, 337–342. doi:10.1159/000108383.
- Kyser, K, 2014. Uranium ore deposits. In: *Treatise on Geochemistry: Second Edition*, 2nd ed. Elsevier Ltd. doi:10.1016/B978-0-08-095975-7.01122-0.
- Larson, L N, Kipp, G G, Mott, H V, Stone, J J, 2012. Sediment pore-water interactions associated with arsenic and uranium transport from the North Cave Hills mining region, South Dakota, USA. *Appl. Geochem.* 27, 879–891. doi:10.1016/j.apgeochem.2012.01.008.
- Lee, M H, Choi, G S, Cho, Y H, Lee, C W, Shin, H S, 2001. Concentrations and activity ratios of uranium isotopes in the groundwater of the Okchun Belt in Korea. *J. Environ. Radioact.* 57, 105–116. doi:10.1016/S0265-931X(01)00014-5.
- Lindsay, M B J, Moncur, M C, Bain, J G, Jambor, J L, Ptacek, C J, Blowes, D W, 2015. Geochemical and mineralogical aspects of sulfide mine tailings. *Appl. Geochem.* 57, 157–177. doi:10.1016/j.apgeochem.2015.01.009.
- MacWilliam, K, 2018. The Geology and Genesis of the Coffee Gold Deposit in West-central Yukon, Canada: Implications for the Structural, Magmatic, and Metallogenic Evolution of the Dawson Range and Gold Exploration Models (Ph.D. thesis). University of British Columbia (497 p. University of British Columbia).
- Mahoney, J J, Cadle, S A, Jakubowski, A T, 2009. Uranyl adsorption onto hydrous ferric oxides - a re-evaluation for the diffuse layer model database. *Environ. Sci. Technol.* 43, 9260–9266. doi:10.1021/es901586w.
- McClelland, J W, Holmes, R M, Peterson, B J, Amon, R, Brabets, T, Cooper, L, Gibson, J, Gordeev, V V, Guay, C, Milburn, D, Staples, R, Raymond, Pa, Shiklomanov, I, Stiegl, R, Zhulidov, A, Gurtovaya, T, Zimov, S, 2008. Development of a Pan-Arctic database for river chemistry from corals to canyons: the Great Barrier Reef Margin. *Program* 89, 217–218. doi:10.1029/2006JG000353.
- Muscattello, J R, Liber, K, 2009. Accumulation and chronic toxicity of uranium over different life stages of the aquatic invertebrate chironomid tentans. *Arch. Environ. Contam. Toxicol.* 57, 531–539. doi:10.1007/s00244-009-9283-1.
- Muscattello, J, Flather, D, Gjertsen, J, 2020. Survival and reproductive effects in the aquatic invertebrate *Ceriodaphnia dubia* exposed to uranium spiked site water collected from two creeks in the Yukon, Canada. *Arch. Environ. Contam. Toxicol.* (In Press). doi:10.1007/s00244-020-00740-z.

- Nordstrom, D K, 2015. Baseline and premining geochemical characterization of mined sites. *Appl. Geochem.* 57, 17–34. doi:10.1016/j.apgeochem.2014.12.010.
- O'Donnell, J A, Aiken, G R, Walvoord, M A, Butler, K D, 2012. Dissolved organic matter composition of winter flow in the Yukon River basin: Implications of permafrost thaw and increased groundwater discharge. *Glob. Biogeochem. Cycles* 26, 1–18. doi:10.1029/2012GB004341.
- Orloff, K G, Mistry, K, Charp, P, Metcalf, S, Marino, R, Shelly, T, Melaro, E, Donohoe, A M, Jones, R L, 2004. Human exposure to uranium in groundwater. *Environ. Res.* 94, 319–326. doi:10.1016/S0013-9351(03)00115-4.
- Paktunc, D, Bruggeman, K, 2010. Solubility of nanocrystalline scorodite and amorphous ferric arsenate: implications for stabilization of arsenic in mine wastes. *Appl. Geochem.* 25, 674–683. doi:10.1016/j.apgeochem.2010.01.021.
- Pichler, T, Mozaffari, A, 2015. Distribution and mobility of geogenic molybdenum and arsenic in a limestone aquifer matrix. *Appl. Geochem.* 63, 623–633. doi:10.1016/j.apgeochem.2015.08.006.
- Plant, J A, Bone, J, Voulvoulis, N, Kinniburgh, D G, Smedley, P L, Fordyce, F M, Klinck, B, 2014. Arsenic and selenium. In: *Treatise on Geochemistry: Second Edition*, 2nd ed. Elsevier Ltd. doi:10.1016/B978-0-08-095975-7.00902-5.
- Post, V E A, Vassolo, S I, Tiberghien, C, Baranyikwa, D, Miburo, D, 2017. Weathering and evaporation controls on dissolved uranium concentrations in groundwater – a case study from northern Burundi. *Sci. Total Environ.* 607–608, 281–293. doi:10.1016/j.scitotenv.2017.07.006.
- Puccia, V, Limbozzi, F, Avena, M, 2015. Arsenic in Porewaters of the unsaturated zone of an argentinean watershed: adsorption and competition with carbonate as important processes that regulate its concentration. *Aquat. Geochem.* 21, 513–534. doi:10.1007/s10498-015-9271-1.
- Reszat, T N, Hendry, M J, 2007. Complexation of Aqueous Elements by DOC in a Clay Aquitard. pp. 1–12. doi:10.1111/j.1745-6584.2007.00338.x.
- Riedel, T, Kübeck, C, 2018. Uranium in groundwater – a synopsis based on a large hydrogeochemical data set. *Water Res.* 129, 29–38. doi:10.1016/j.watres.2017.11.001.
- Rosen, M R, Burrow, K R, Fram, M S, 2019. Anthropogenic and geologic causes of anomalously high uranium concentrations in groundwater used for drinking water supply in the southeastern San Joaquin Valley, CA. *J. Hydrol.* 577, 124009. doi:10.1016/j.jhydrol.2019.124009.
- Rudnick, R L, Gao, S, 2014. Composition of the continental crust. In: *Treatise on Geochemistry: Second Edition*, 2nd ed. Elsevier Ltd. doi:10.1016/B978-0-08-095975-7.00301-6.
- Ryan, J.J., Zagorevski, A., Williams, S.P., Roots, C., Giolkiewicz, W., Hayward, N., Chapman, J.B., 2013. Geology, the Stevenson Ridge (Northeast Part), Yukon; Geological Survey of Canada, Canadian Geoscience Map 116 (2nd Edition, Preliminary), Scale 1:100 000. <https://doi.org/10.4095/292407>.
- Ryan, J J, Zagorevski, A, Piercey, S J, 2018. Geochemical Data of Yukon-Tanana and Slide Mountain Terranes and Their Successor Rocks in Yukon and northern British Columbia. *Geol. Surv. Canada, Open File 8500* (doi:10/4095/313250).
- Saalfield, S L, Bostick, B C, 2010. Synergistic effect of calcium and bicarbonate in enhancing arsenate release from ferrihydrite. *Geochim. Cosmochim. Acta* 74, 5171–5186. doi:10.1016/j.gca.2010.05.022.
- Salminen, R, Batista, M J, Bidovec, M, Demetriades, A, De Vivo, B, De Vos, W, Duris, M, Gilucis, A, Gregorauskiene, V, Halamic, J, Heitzmann, P, Lima, A, Jordan, G, Klaver, G, Klein, P, Lis, J, Locutura, J, Marsina, K, Mazreku, A, O'Connor, P, J, Olsson, SÅ, Ottesen, R-T, Petersell, V, Plant, J A, Reeder, S, Salpeteur, I, Sandström, H, Siewers, U, Steenfelt, A, Tarvainen, T, 2006. *Geochemical Atlas of Europe. Part 1: Background Information, Methodology and Maps*.
- Selby, D, Nesbitt, B E, 2000. Chemical composition of biotite from the casino porphyry Cu-Au-Mo mineralization, Yukon, Canada: Evaluation of magmatic and hydrothermal fluid chemistry. *Chem. Geol.* 171, 77–93. doi:10.1016/S0009-2541(00)00248-5.
- Smedley, P L, Kinniburgh, D G, 2002. A review of the source, behaviour and distribution of arsenic in natural waters. *Appl. Geochem.* 17, 517–568.
- Smedley, P L, Smith, B, Abesser, C, Lapworth, D, 2006. Uranium occurrence and behaviour in British groundwater. *Br. Geol. Surv. Groundw. Program. Comm. Rep. (CR/06/050N 48)*.
- Smith, L C, Sheng, Y, MacDonald, G M, 2007. A first pan-Arctic assessment of the influence of glaciation, permafrost topography and peatlands on northern hemisphere lake distribution. *Permafrost. Periglac. Process.* 18, 201–208. doi:10.1002/ppp.
- Sracek, O, Bhattacharya, P, Jacks, G, Gustafsson, J P, Von Brömssen, M, 2004. Behavior of arsenic and geochemical modeling of arsenic enrichment in aqueous environments. *Appl. Geochem.* 19, 169–180. doi:10.1016/j.apgeochem.2003.09.005.
- Stewart, B D, 2008. *The Dominating Influence of Calcium on the Biogeochemical Fate of Uranium*. Stanford University.
- Stewart, B D, Mayes, M A, Fendorf, S S, 2010. Impact of complexes on uranium(VI) adsorption to synthetic and natural sediments. *Environ. Sci. Technol.* 44, 928–934.
- Stewart, B D, Amos, R T, Nico, P S, Fendorf, S, 2011. Influence of uranyl speciation and iron oxides on uranium biogeochemical redox reactions. *Geomicrobiol J.* 28, 444–456. doi:10.1080/01490451.2010.507646.
- Striegl, R G, Aiken, G R, Dornblaser, M M, Raymond, P A, Wickland, K P, 2005. A decrease in discharge-normalized DOC export by the Yukon River during summer through autumn. *Geophys. Res. Lett.* 32. doi:10.1029/2005GL024413.
- Tixier, K, Beckie, R, 2001. Uranium depositional controls at the Prairie Flats surficial uranium deposit, Summerland, British Columbia. *Environ. Geol.* 40, 1242–1251. doi:10.1007/s002540100303.
- Toohay, R C, Herman-Mercer, N M, Schuster, P F, A, M E, Koch, J C, 2016. Multidecadal increases in the Yukon River Basin of chemical fluxes as indicators of changing flowpaths, groundwater, and permafrost. *Geophys. Res. Lett.* 120–130. doi:10.1002/2016GL070817.
- Vriens, B, Skierszkan, E K, St-Arnault, M, Salzsauler, K, Aranda, C, Mayer, K U, Beckie, R D, 2019. Mobilization of metal(oid) oxyanions through circumneutral mine waste-rock drainage. *ACS Omega* 4, 10205–10215. doi:10.1021/acsomega.9b01270.
- Wainwright, A J, Simmons, A T, Finnigan, C S, Smith, T R, Carpenter, R L, 2010. Geology of new gold discoveries in the Coffee Creek area, White Gold District, west-central Yukon. *Yukon Explor. Geol.* 233–248.
- Waite, T D, Davis, J A, Payne, T E, Waychunas, G A, Xu, N, 1994. Uranium(VI) adsorption to ferrihydrite: application of a surface complexation model. *Geochim. Cosmochim. Acta* 58, 5465–5478. doi:10.1016/0016-7037(94)90243-7.
- Walvoord, M A, Striegl, R G, 2007. Increased groundwater to stream discharge from permafrost thawing in the Yukon River basin: potential impacts on lateral export of carbon and nitrogen. *Geophys. Res. Lett.* 34. doi:10.1029/2007GL030216.
- Welch, A H, Lico, M S, 1998. Factors controlling As and U in shallow ground water, Southern Carson Desert, Nevada: RN - *Appl. Geochem.*, v. 13, p. 521–539. *Appl. Geochem.* 13, 521–539.
- Wu, Y, Wang, Y, Xie, X, 2014. Occurrence, behavior and distribution of high levels of uranium in shallow groundwater at Datong basin, northern China. *Sci. Total Environ.* 472, 809–817. doi:10.1016/j.scitotenv.2013.11.109.
- Yukon Environment Geomatics Traditional territories of Yukon First Nations and Settlement Areas of Inuvialuit and Tetlit Gwich'in. Map ID:ENV.020.01 [WWW Document]. URL http://www.env.gov.yk.ca/animals-habitat/documents/traditional_territories_map.pdf 201315 July 2019
- Yukon Geological Survey Regional geochemical survey re-analysis [WWW Document] URL <http://data.geology.gov.yk.ca/Compilation/21201612> January 2018
- Zamora, M L L, Zielinski, J M, Moodie, G B, Dcbr, R A F F, Dcbr, W C H, Capello, K, 2010. Uranium in drinking water: renal effects of long-term ingestion by an aboriginal community. *Arch. Environ. Occup. Health* 64, 228–241. doi:10.1080/19338240903241267.